Eur. Phys. J. E **14**, 269–276 (2004)
DOI 10.1140/epje/i2003-10151-2

THE EUROPEAN PHYSICAL JOURNAL E

# Hemifusion and fusion of giant vesicles induced by reduction of inter-membrane distance

J. Heuvingh[1,a], F. Pincet[2], and S. Cribier[1]

[1] Laboratoire de Physico-Chimie Moléculaire des Membranes Biologiques, URD-CNRS UMR 7099, IBPC, 13 rue Pierre et Marie Curie, 75005 Paris, France
[2] Laboratoire de Physique Statistique, ENS, 24 rue Lhomond 75231 Paris cedex 05, France

Received 22 July 2003 and Received in final form 26 May 2004 /
Published online: 3 August 2004 – © EDP Sciences / Società Italiana di Fisica / Springer-Verlag 2004

**Abstract.** Proteins involved in membrane fusion, such as SNARE or influenza virus hemagglutinin, share the common function of pulling together opposing membranes in closer contact. The reduction of inter-membrane distance can be sufficient to induce a lipid transition phase and thus fusion. We have used functionalized lipids bearing DNA bases as head groups incorporated into giant unilamellar vesicles in order to reproduce the reduction of distance between membranes and to trigger fusion in a model system. In our experiments, two vesicles were isolated and brought into adhesion by the mean of micromanipulation; their evolution was monitored by fluorescence microscopy. Actual fusion only occurred in about 5% of the experiments. In most cases, a state of "hemifusion" is observed and quantified. In this state, the outer leaflets of both vesicles' bilayers merged whereas the inner leaflets and the aqueous inner contents remained independent. The kinetics of the lipid probes redistribution is in good agreement with a diffusion model in which lipids freely diffuse at the circumference of the contact zone between the two vesicles. The minimal density of bridging structures, such as stalks, necessary to explain this redistribution kinetics can be estimated.

**PACS.** 87.16.Dg Subcellular structure and processes: Membranes, bilayers, and vesicles – 87.15.Vv Biomolecules: structure and physical properties: Diffusion – 64.70.Nd Structural transitions in nanoscale materials

## 1 Introduction

Membrane fusion is a topic of essential interest in diverse areas of biological science, such as transport inside the cell, viral infection, delivery of hormones and neurotransmitters, or fertilization. In the recent years, progresses have been achieved in the description and understanding of the molecular machinery of membrane fusion. For intracellular transport, SNARE proteins are believed to be responsible for fusion. Reconstituted in artificial vesicles in the absence of any other protein, their presence was sufficient to promote fusion [1].

SNARE proteins in opposing membranes can interact, forming a SNAREpin, and pulling together the membranes in which they are embedded. The reduction of inter-membrane distance could directly induce a transition state of the phospholipids [2] triggering fusion. A mechanical effect of the SNAREs could also be involved in the merging of the distal monolayers [3]. Another hypothetical pathway to fusion [4] reduces the role of lipids and involves primarily proteins as constituents of the initial fusion pore leading to fusion.

Viral fusion proteins are believed to trigger fusion between the virus and the host cell membrane by a similar mechanism of pulling membranes together [5,6].

The aim of this work is to mimic these systems in an entirely artificial protein-free system, by bringing the membranes of two vesicles into closer contact and show that lipid layers alone can fuse or partly fuse. More precisely, we will point out that if the lipid layers are brought close enough to each other, fusion or an intermediate state called hemifusion can occur. The idea of studying hemifusion or fusion in model systems by the reduction of inter-membrane distance induced by dehydration is not new. For example, dehydration has been either directly induced [7] or mediated by poly(ethylene glycol) [8]. However, some quantitative features are difficult to control and measure in these systems (*e.g.*, tension, dynamics of the lipid redistribution, volume and membrane surface variations, initial time of contact between the membranes, ...). The use of giant unilamellar vesicles allows to circumvent most of these difficulties.

[a] e-mail: julien.heuvingh@univ-paris5.fr

The forces applying in the interaction between two lipidic membranes are: the van der Waals attraction, the double layer electrostatic repulsion between the zwiterionic lipids, the repulsion by Helfrich's thermal undulation [9], and several short-range repulsion forces (hydration, protrusion, steric hindrance) [10,11]. For membranes of dioleoyl-phosphocholine, a separation distance of 3 nm was measured by X-ray diffraction by Rand and Parsegian [12]. By adding in our system functionalized lipids bearing the DNA bases thymidine or adenosine as headgroups, we introduce a supplementary force (the H-bond between nucleosides), enhancing attraction between the membranes. Numerical estimation of the interaction energy as a function of the intermembrane distance shows a decrease of the equilibrium distance from 3 nm without the supplementary force to 1 nm with the supplementary force (calculated by Pincet *et al.* [13]). The interaction between the nucleosides lipid derivative and their behavior have been previously described [14]. The decrease of the intermembrane distance is only effective where the specific force is applying, *i.e.* where two functionalized lipids, or stacks of functionalized lipids [15] from the membranes come into vicinity. The membranes might therefore be 3 nm distant, with patches of membrane protruding toward each other. Such a protrusion is similar to the deformation observed in exocytosis [16] that may be induced by fusogenic proteins [17]. It has also been theoretically shown that these protrusions facilitate the formation of stalk intermediates between two bilayers [18]. When stalks are formed, the topological structure of the membranes is similar to the commonly called hemifusion state where the contacting leaflets of both bilayers have merged whereas the inner leaflets remain independent. Such stalk structures have recently been observed by X-ray diffraction [7].

## 2 Materials and methods

### 2.1 Materials

The functionalized lipids with thymidine or adenosine as headgroups (later referred to as adenosine or thymidine lipids) were obtained by coupling the unprotected nucleosides to 2-(1,3-dioleyloxy) propylhemisuccinic acid using a modified DCC/DMAP method [19]. Dioleoyl-*sn*-phosphatidylcholin (DOPC), fluorescein isothiocyanate dextran (MW: 9300kDa) and bovine albumin were purchased from SIGMA. 1,2-dioleoyl-*sn*-glycero-3-phosphoethanolamine-N-(lissamine rhodamine B sulfonyl) (RhPE) was purchased from Avanti Polar Lipids. Vitrex sigilium paste was purchased from Modulohm A/S (Herlev, Denmark). Coated ITO glass was purchased from Thales Electron Device (Vélizy, France).

### 2.2 Preparation of GUV

Giant unilamellar vesicles were produced by the electroformation method [20]. Briefly, the preparation chamber is made of two glass plates coated with an indium tin oxide (ITO) film, which renders them conductive. Phospholipids were dissolved in chloroform/methanol (5/3). For each sample, 10 $\mu$g were carefully deposited as homogenous pitch on the conductive side of each glass plate. They were then put under vacuum for 1 hour in order to eliminate the remaining solvent. The two plates with the conductive faces opposing each other, together with a 1 mm thick Teflon spacer form a 2ml chamber, which is sealed with sigillum paste. The chamber is filled with a 300 mM sucrose solution. An AC field (8 Hz) was then applied between the two plates of the chamber, quickly after the filling, in order to prevent the spontaneous formation of vesicles. The lipid film swelled as the electric voltage was progressively increased to 1 volt over one hour, remaining at this value overnight. The giant vesicles are finally detached from the glass plate by the application of an electric AC tension of higher voltage and shorter period (4 Hz). The vesicles used for the experiments were directly taken from the preparation chamber with a capillary pipette inserted through a hole in the Teflon spacer. Giant vesicles prepared in this manner are mostly unilamellar [21].

The osmolarity of each solution used in these experiments was carefully checked with a micro-osmometer (Roebling, Germany). The glucose and sodium chloride solutions in which the vesicles were observed were adjusted at a slightly higher osmolarity than the swelling sucrose solution, in order to deflate the vesicles. This is required for pipette holding and to obtain a suitable contact area during aggregation of the vesicles.

### 2.3 Observation of liposomes and micromanipulation

Liposomes were observed by epi-fluorescence and phase contrast optical microscopy, using an inverted microscope (Zeiss IM35). The objective lens was X32 (N.A. 0.40, Zeiss, Germany). The fluorescence was excited by an argon laser (Coherent Innova 90-4) tuned at 514 nm (green) for rhodamine-labeled lipids and at 488 nm (blue) for fluorescein-labeled dextran. The images were acquired on a Micromax 5 MHz digital camera (Roperscientific, USA) with a PI 782 $\times$ 582 Interline CCD Array.

Transfer micromanipulation was used in order to maneuver independent vesicles and to transfer vesicles from a stock chamber to an observation chamber where the conditions were well defined. The micromanipulation device was made up of two micromanipulators (Leitz, Germany) and three pipette holders (Narishige, Japan). Two types of micropipettes were used: small suction pipettes (internal diameter 5–10 $\mu$m) and larger transfer pipettes (internal diameter 100–300 $\mu$m). The aspiration was controlled by hydrostatic pressure up to 500 Pa. The transfer pipette was made and used as indicated by Kwok and Evans [22].

The micromanipulation chamber was made up of two metal plates and four thin glass slides. The glass slides formed two independent parallel chambers of approximately 300 $\mu$l, into which the solutions stand by capillarity on two sides, allowing pipettes to enter the solution or to pass through it. The two chambers along with the pipettes

were incubated in a solution of 10% BSA in pure water during one hour to prevent adhesion of vesicles with the pipettes or glass slide, and were then emptied and rinsed out twice from the solution. One of the chambers (the stock chamber) was then filled with a 310 mOsm glucose solution, the other one (the observation chamber) with a 320 mOsm NaCl solution. The vesicles were put in the stock chamber with a capillary pipette. The vesicles sunk to the bottom of the chamber in a few minutes, due to the density difference between the sucrose solution inside the vesicle and the glucose solution outside. We selected a suitable vesicle and held it by a suction pipette. It was then transferred and put down on the bottom of the observation chamber. This operation was repeated with another vesicle of the appropriate type and of similar size. The second vesicle was placed near the first one. A flow was then set by a pipette aspiration in order to displace the two vesicles, and to bring them into contact.

### 2.4 Fluorescence quantification

For quantification purpose, we usually determined the mean density of fluorescence probes on a vesicle. A rectangular selection was chosen around the center of the vesicle's projected image. The intensity of the fluorescence signal in the selection was averaged, and we took as error bars the standard deviation of the fluorescence intensity in the selection. This choice of selection allowed us to avoid errors due to a higher projection of the membrane closer to the border, and to the drift caused by the polarization of the laser light source and by the mean orientation of the dipolar momentum of probes in the membrane. This quantification was done with the *Image J* software, provided by the National Institute of Health (USA).

## 3 Results and discussion

### 3.1 Observation

In a first set of experiments we used two types of vesicles, both predominantly made of DOPC. The first type contained a fixed amount of adenosine lipids (ranging from 1% to 10% of the total lipids), and 2% RhPE as fluorescent label. The second type bore thymidine lipids (same amount as adenosine on the former type), and had no fluorescence apart from the intrinsic fluorescence of DOPC. This intrinsic fluorescence is at least 5 orders of magnitude smaller than the RhPE fluorescence. Two vesicles of different types were selected from the stock chamber and transferred to the observation chamber. The two vesicles were then brought into close proximity. Aggregation of the vesicles (deformation with formation of an adhesion area between the vesicles) happened spontaneously within minutes or was triggered by displacing the vesicles with a flow of the pipette.

Immediately after aggregation (within 5 seconds, the time resolution of the experimental setup), a fluorescent signal was observed on the non-labeled vesicle. During a few minutes the fluorescence intensity on the thymidine-bearing vesicle increased, while the fluorescence intensity decreased on the adenosine-bearing vesicle. In most of the experiments an equilibrium, stable for several hours, was reached.

In five percent of the experiments (7 occurrences), the vesicles collapsed, forming a bigger one. In the other cases, the fluorescence transfer reached equilibrium. These observations and their kinetics were the same for vesicles containing 1, 2, 5 and 10% of functionalized lipid (adenosine and thymidine).

Control experiments were conducted with vesicles containing neither adenosine nor thymidine lipids. The aggregation was still observed, but no fluorescence transfer was detected over more than an hour, in agreement with results of Pincet *et al.* [13]. No collapse of two vesicles into a bigger one was observed during control experiments.

### 3.2 Equilibrium

When an equilibrium was reached, the fluorescence intensity of the formerly non-fluorescent vesicle was still inferior to the intensity of the formerly fluorescent vesicle (see Fig. 1).

#### 3.2.1 Hemifusion

The relative difference in the fluorescence of the two vesicles at equilibrium suggests that the system may have reached a state known as hemifusion state where the contacting leaflets of both bilayers have merged whereas the inner leaflets (as well as the interior of the vesicles) remain independent. This can be shown in three complementary ways: i) by directly quantifying the fluorescence ratio of the vesicles at equilibrium; ii) by labeling the aqueous content of one vesicle; and iii) by trying to separate the vesicles. The results of these three approaches are described in this section.

Fluorescence microscopy images were recorded and analyzed to compare the fluorescence intensity on the membrane of both vesicles, after transfer has reached equilibrium. The ratio of fluorescence between the two vesicles (*i.e.* the fluorescence density on the formerly non-fluorescent vesicle divided by the fluorescence density on the formerly fluorescent vesicle) was collected for about fifty couples of vesicles. This ratio was found to be close to one third for vesicles of the same size. In the case of hemifusion, this result is expected, as the fluorescent markers on the outer leaflet of the originally labeled vesicle redistributed between the two vesicles, whereas the markers of the inner leaflet stay in the membrane of the originally labeled vesicle. The expected fluorescence ratio for vesicles of different size enduring hemifusion is calculated in Appendix A. The experimental equilibrium transfer ratio is found to be very close to the calculated theoretical ratio, denoting a lipid mixing of the outer leaflets of both vesicles, without the mixing of inner leaflets (see Fig. 2).

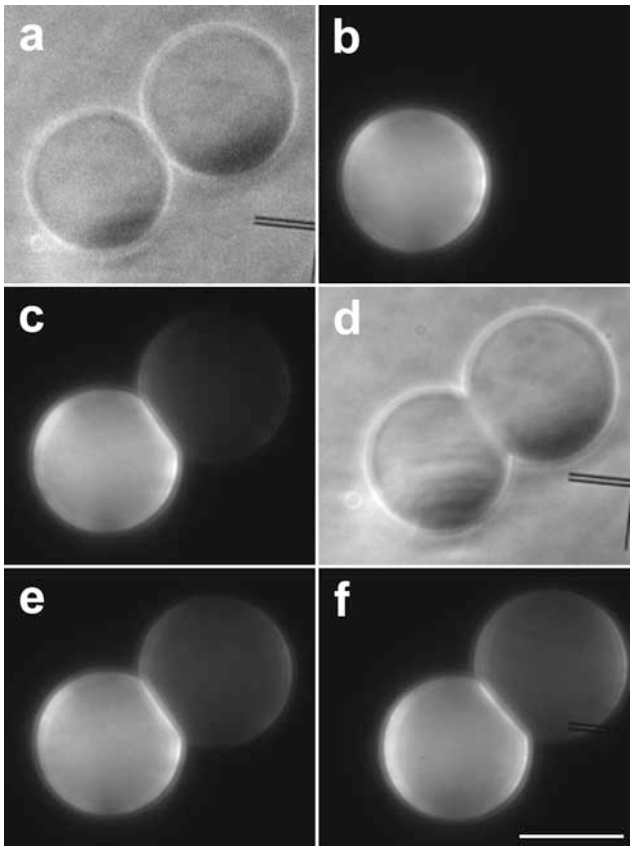


**Fig. 1.** Two tangent vesicles seen by phase contrast microscopy (a) and epi-fluorescence (b). One of the vesicles is functionalized by adenosine lipids and labeled by RhPE, the other one is functionalized by thymidine lipids. Just after aggregation of the two vesicles, as attested by membrane deformation in the contact area (d), a fluorescent signal appeared on the non-labeled vesicle (c), denoting a lipid mixing. Fluorescent lipids carry on their redistribution after 3 minutes (e) until they reached equilibrium after 6 minutes (f). The fluorescence density on the thymidine-bearing vesicle was still inferior to the fluorescence density of the adenosine-bearing vesicle. The bar is 20 $\mu$m.

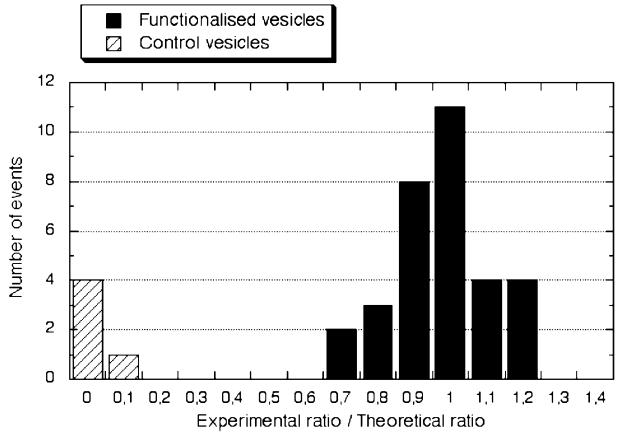


**Fig. 2.** Comparison between experimental and theoretical ratio of fluorescence density between the two vesicles, after redistribution has reached an equilibrium. The experimental ratio is the fluorescence density measured on the formerly non-fluorescent vesicle divided by the fluorescence density measured on the formerly fluorescent vesicle. The theoretical ratio of two vesicles enduring a mixing of their outer monolayer, but no mixing of their inner monolayer, was calculated according to Appendix A. For vesicles' couple containing adenosine and thymidine lipids, the experimental ratio is close to the theoretical one. For control vesicles bearing no functionalized lipids the experimental ratio is close to zero (no lipid redistribution).

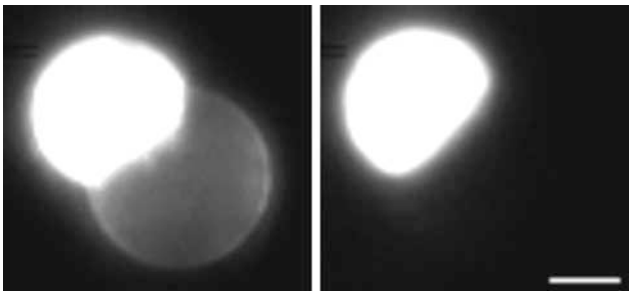

**Fig. 3.** Two aggregated vesicles. One of the vesicles is functionalized by adenosine lipids and labeled by RhPE on surface and by FITC-dextran in volume; the other one is functionalized by thymidine lipids. Fluorescence imaging with a laser tuned on the excitation wavelength of rhodamine (514 nm) shows lipid mixing (left). Fluorescence imaging with a laser tuned on the excitation wavelength of fluoresceine (488 nm) shows no aqueous content mixing (right). The bar is 10 $\mu$m.

In a separate set of experiments, we grew the adenosine fluorescent vesicles in a fluorescent solution. The solution contained 1 mM dextran (9300 Da) labeled with fluorescein. Sucrose was added in order to maintain a 300 mOsm osmolarity. The vesicles are therefore fluorescently labeled on their surface by rhodamine and in volume by fluoresceine. These vesicles, along with thymidine vesicles, were as previously put in the stock chamber, and transferred to the observation chamber. The dextran concentration was set to give a fluorescence emission one order of magnitude stronger than the membrane emission. As the vesicles aggregated, fluorescence emissions were checked on the thymidine vesicle with the laser set alternatively on the fluorescein absorption wavelength (488 nm) and on the rhodamine absorption wavelength (514 nm). Minutes after aggregation, a good fluorescent rhodamine signal was seen on the thymidine vesicle, denoting lipid mixing, but no fluorescence signal was detected for the fluorescein absorption wavelength more than one hour after lipid mixing (see Fig. 3). Therefore, if any leakage had occurred during this time, it was below the resolution of our system (less than one percent of the fluorescent dextran leaked to the other vesicle). This denotes a lack of significant content mixing, at least for molecules with a radius of more than 3 nm [23].

Finally, when we tried to separate the vesicle doublet after equilibrium was reached, we were not able to revert it to two completely independent vesicles. This was checked by holding tightly both vesicles by pipettes with a high suction pressure. Provided that the vesicles were not destroyed by the mechanical stress, the pipettes were pulled

apart. The vesicles seemed then completely separated in phase contrast microscopy. This result gives a strong indication that both vesicles still have distinct interior media.

In reality, this separation was not complete since a lipid filament (tether) of unknown structure could still be seen linking the vesicles by fluorescence. When one of the vesicles was released, it hurled back toward the other vesicle, indicating strong tension in the tether. However, this tether is not characteristic of hemifusion as has already been observed before in adhering systems [24]. This was confirmed in control experiments where two adhering vesicles containing neither adenosine nor thymidine lipids were separated.

These three different approaches show unambiguously that hemifusion is indeed reached in our system: the outer leaflets are shared while the inner leaflets, as well as the interior of the vesicles, are completely distinct.

### 3.2.2 The decrease in separation distance triggers hemifusion

The physical factor that triggers hemifusion has also to be discussed. Since the functionalized lipids are able to decrease the equilibrium distance between adhering bilayers from 3 nm down to 1nm, the hydration of the lipids in the contact area tends to be smaller than its most favorable one [25]. This process is similar to what happens when pushing on membranes very strongly. It has already been observed that supported membranes that were pushed against each other with high forces were indeed able to hemifuse [26]. These experiments showed that fusion needs less force to be achieved when the contact area is more depleted in lipids [26,27]. A recent paper by Safran [28] showed how the decrease of lipid density in the contact area can induce hemifusion. With our functionalized molecules, the lipids in the contact area are frustrated by the dehydration. Therefore, their chemical potential becomes higher than the one in the non-frustrated state before adhesion and, since they have to equilibrate with the lipids in the outer region, there must be a slight depletion to equalize the chemical potentials. This depletion would expose the hydrophobic parts of the lipids and could produce hemifusion.

### 3.2.3 Structure of the contact zone

Even though the hemifusion state is clearly established, the organization of the lipids in the contact area remains unknown. In other terms, the intermediary state toward fusion in which the system is blocked still has to be elucidated. The structure of the contact zone remains unclear.

When two vesicles endure hemifusion, the membranes in the contact area must rearrange from a bilayer to another structure. The model currently favored for the fusion of purely lipidic membranes is the stalk hypothesis [29, 30]. In this model, the first intermediary state toward fusion is the formation of a thin lipid bridge (stalk) linking the two outer monolayers. A slight evolution of the stalk structure would then allow a contact between the two inner monolayers. Two scenarios are proposed to go from the stalk intermediate to the formation of a pore in the membrane, leading to fusion. The first one is the direct formation of a pore. The second one is the enlargement of the stalk, creating a diaphragm, *i.e.* a bilayer formed by the inner monolayers of both vesicles. Destabilization of the diaphragm would then trigger pore formation.

According to this stalk hypothesis, the structure of the contact area of the hemifused doublets in our experiments could be either a stalk structure or a diaphragm. However, the picture of a diaphragm spanning the whole contact area seems unrealistic at such scales (the typical contact area of the two giant vesicles is hundreds of square microns). In particular, the very high elastic modulus (about 0.1 N/m for a vesicle membrane [31]) prevents such a high compression of the membrane, which means there is no space for the lipids of the outer membranes to be driven away from the interface. We tried to get direct evidence of the presence of two bilayers at the interface, instead of the single diaphragm bilayer. Unfortunately, quantification of the straight vertically oriented contact area proves difficult to obtain in a convincing way. However, no fluorescence loss of the interface was observed between images taken immediately before and after the start of the hemifusion (data not shown).

We can therefore, with reasonable confidence, hypothesize that the structure of the contact area is a stalk structure with a sufficient number of stalks or of equivalent "bridging structures" which could be, for instance, diaphragms of limited extent.

Since the lipids have to pass through these bridging structures, it can be suspected that their diffusion would be slowed down during their transfer from one vesicle to the other. This could be checked by directly quantifying the kinetics of fluorescence redistribution. Fluorescence ratios were compiled for different times before equilibrium was reached. In this way, we obtained the kinetics of the lipid redistribution between the two hemifused vesicles. This kinetics was compared to a model for lipid redistribution based on Rubin *et al.* [32] where the outer membrane's lipids freely diffuse on the surface of two truncated spheres picturing the hemifused doublet (see Fig. 4). This model will thereafter be referred as the "peanut model", because of its geometrical aspect. We numerically solve the diffusion equation in this geometry (see App. B) with a diffusion coefficient of 3 $\mu m^2/s$ [33]. The redistribution of lipids can then be predicted, given only the radius of the vesicles and the contact angle between them. The experimental kinetics of redistribution compare very well with the model kinetics for all vesicles' couples (see Fig. 5) showing that the lipid diffusion is not significantly slowed down during their transfer from one vesicle to the other. This indicates that there must be a sufficient number of bridging structures for the lipids reaching the contact area to rapidly get into a stalk as they diffuse on the interface, and cross it to the other vesicle. A lower bound of the stalks density can be roughly estimated by analogy with the so-called "trap model" [34] which gives the relation between this density

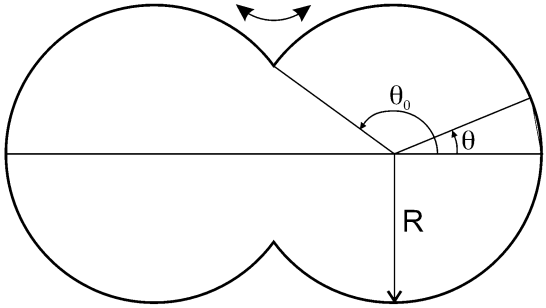


**Fig. 4.** Schematic drawing of the cross-section of the outer monolayer of a vesicle couple enduring unrestricted hemifusion. This model geometry is used to calculate the kinetics of lipid probe redistribution. At time 0, all lipid probes are located on the left vesicle. The partial derivative diffusion equation is numerically solved in this geometry (see App. B).

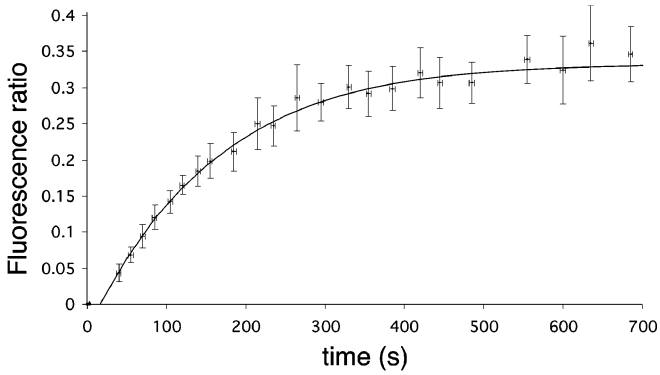


**Fig. 5.** Typical kinetics of lipid redistribution in a functionalized vesicles' couple. Fluorescence ratios between the two vesicles were measured during lipid redistribution. The curve is derived from the numerical calculation of a model of diffusion on the surface of two truncated spheres, using the dimensions of both vesicles ($R = 14.1$ $\mu$m, $\theta_0 = 2.3$ rad). The curve encompasses all experimental points within their error bars. Note that this curve is not a fit but the expected one from the experimentally measured diffusion coefficient $D$ (3 $\mu m^2 s^{-1}$ [33]). Time 0 is defined as the time of the last measure before the start of a detectable fluorescence transfer (start of hemifusion) and the theoretical curve is slightly translated in time (within the 20 seconds for the start of the fluorescence transfer) to match the experimental data.

and the delay in the diffusion caused by the presence of the stalks. As we know this delay is smaller than the experimental error, this model shows that very few stalks per 100 $\mu m^2$ would be sufficient to explain the experimental results. This result may seem surprising; however, it has to be remembered that the lipids have a very high diffusion coefficient (3 $\mu m^2 s^{-1}$) meaning that they cover 10 $\mu m^2$ in about 3 s. As stalks could be structures with a short lifetime [30], this estimate has to be considered as the minimal amount required at a given time.

Since all proportions of functionalized lipids down to one percent lead to an agreement between the "peanut model" and the experiment, it is likely that the number of stalks present at the interface between two vesicles bearing ten percent of functionalized lipids is larger. Some authors have proposed an alternative to the stalks in which there would be transverse diffusion of lipids where the hydrophobic tails cross the water gap between the membranes to explain lipid exchange [35]. Such a transfer cannot be present in our system as the characteristic time of lipid residence in a bilayer is at least three orders of magnitude greater [10] than what we observed.

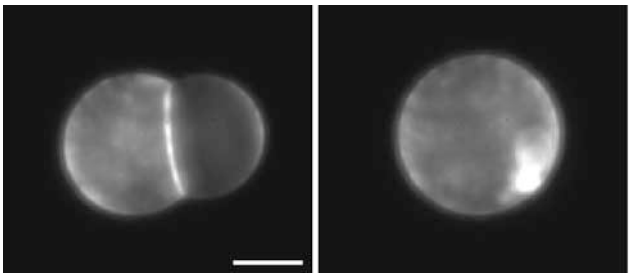

**Fig. 6.** Fluorescence images of a hemifused doublet enduring full fusion. The two original vesicles (left) and the resultant vesicle (right) are seen by fluorescence microscopy. The internal volume is conserved during the transformation. The total area of the membrane is not conserved; a highly fluorescent region, probably due to an aggregate of supernumerary lipids, can be seen inside the resultant vesicle. The bar is 10 $\mu$m.

### 3.3 Fusion

The collapse of two adhering vesicles in one spherical vesicle (see Fig. 6) is a fusion process. In the fusion events that were observed, fusion frequency did not seem to depend on the functionalized lipid concentration. In all cases, the resulting vesicle was also spherical, indicating that either some outer medium had entered the final vesicle (increase in the total volume) or part of the membrane was not any more present on the spherical surface (decrease of the total area). The contrast between inner and outer medium was still present, showing that no major leakage took place in the process. This is confirmed by direct measurement of the vesicles radii before and after fusion. The volume of the resultant vesicle was always very similar (less than ten percent increase) to the sum of the volume of the two original vesicles. The total area was never conserved during fusion. The excess of membrane is observable inside the resultant vesicle (see Fig. 6). It can be located in invaginations or in lipidic aggregates.

Tension of the vesicle membranes is often claimed to play a role in fusion processes [36]. In our system, the adhesion of the vesicles induces a tension of at least $10^{-5}$ N/m (this latter corresponds to the tension between two pure DOPC vesicles). To test the role of tension, in several occasions, we induced a tension of about $5 \cdot 10^{-4}$ N/m to both vesicles enduring hemifusion, with suction micropipettes. This did not trigger any fusion, even though it lies within the regime where the membranes are highly stretched [22].

The process of the full fusion of two giant vesicles was an unintuitive result, as conservation of both volumes and

areas would have led to an unstable non-spherical resultant vesicle. Actually, this irreversible process seems to favor volume conservation, characteristic for a fusion without leakage.

## 4 Conclusion

Transfer micromanipulation offers many improvements from usual experiments. First, it allowed us to study an independent vesicles' couple without any aggregation of supernumerary giant vesicles. We also avoided the aggregation of sub-micronic vesicles (LUV or SUV produced concomitantly with GUV by the electroformation method) which could increase the fluorescence signal on both giant vesicles.

For aqueous content labeling of the vesicles, we grew the GUV in a highly concentrated fluorescent dextran solution. When a vesicle sample was put in the deposit chamber, a high fluorescent background was present, due to the diluted fluorescent dextran solution. Transfer to the observation chamber allowed us to avoid this background, which would have hampered our measurements.

The approach presented here allowed to observe fusion and a fusion intermediate, hemifusion, triggered by the addition of short-range specific forces in a couple of purely lipidic giant vesicles. Even though the fusion events did not occur very often, their frequency is sufficiently high (5%) for this system to be used as a fusion model in aqueous media. This result widens the field of applications of model systems to full fusion studies.

For hemifusion, accordance between the observed and calculated ratios of fluorescence of the two vesicles, after lipid redistribution reached equilibrium, along with the absence of redistribution of an aqueous dye, allowed us to identify this fusion intermediate as hemifusion. The redistribution kinetics of lipid probes (in accordance with our diffusion model) is compatible with a stalk structure of the contact zone, provided there is a sufficient number of stalks. This intermediate is stable over hours in most cases, although destabilization leaded to full fusion in a limited number of experiments. The absence of coupling between the proximal and distal leaflets could be responsible for the scarceness of full fusion events in our system [3,37].

The authors wish to thanks Jean-Philippe Bouchaud for useful discussions about convective effects in diffusion and Eric Brunet for his help in the numerical solving of diffusion equations. J.H. was recipient of a fellowship from the Ministère de l'Education, de la Recherche et de la Technologie.

## Appendix A. Theoretical fluorescence ratio for vesicles of different sizes

Let $N$ be the total number of fluorescent labels on the vesicle, $A_1$ and $A_2$ the areas of the initially fluorescent and initially non-fluorescent vesicles. In the case of hemifusion, after equilibrium is reached, half of the fluorescent labels are still present in the inner monolayer of the initially fluorescent vesicle, whereas the other half is divided between the outer monolayers of both vesicles. The surface densities of fluorescent probes on the vesicles are therefore proportional to

$$F_1 \propto \frac{1}{2}\frac{N}{A_1} + \frac{1}{2}\frac{N}{(A_1+A_2)}\,,$$
$$F_2 \propto \frac{1}{2}\frac{N}{(A_1+A_2)}\,.$$

Hence the fluorescence ratio between the vesicles is

$$R = \frac{F_2}{F_1} = \frac{A_1}{2A_1+A_2}\,.$$

By measuring the radius of both vesicles, we can therefore predict their theoretical fluorescence ratio, when the vesicles endure hemifusion, and after the complete redistribution of the lipids.

## Appendix B. Model for the kinetics of lipid's redistribution

In this model, the outer membrane's lipids freely diffuse on the surface of two truncated spheres picturing the hemifused doublet (see Fig. 6). On each vesicle, the surface density of fluorescent probes $C(\theta,t)$ obeys the spherical diffusion equation:

$$\frac{\partial C}{\partial t} = \frac{D}{R^2}\frac{1}{\sin\theta}\frac{\partial}{\partial\theta}\left(\sin\theta\frac{\partial C}{\partial\theta}\right)\,, \quad 0\leqslant\theta\leqslant\theta_0\,, \qquad \text{(B.1)}$$

where $D$ is the lateral diffusion coefficient for PE probes in DOPC at 20 °C, $R$ the radius of the vesicle and $\theta_0$ the contact angle between the two vesicles. The surface density and the diffusive flux must be continuous at the junction of the two vesicles. The surface density at $t=0$ is equal to the initial concentration $C_0$ per monolayer on the initially fluorescent vesicle and to zero on the other vesicle.

For vesicles of the same size, the problem is symmetrical with respect to the plane where the vesicles join. As the two diffusion equations are linear, the difference $M(\theta,t)$ between the surface density at two symmetrical points on the sphere obeys the diffusion equation (B.1). The sum of the surface density at these points, which also obeys equation (B.1), is always equal to the initial concentration $C_0$. Continuity of the surface density at the junction imposes $M(\theta_0,t)$ to be null at all times.

Given the partial differential equation (B.1), the initial and boundary conditions, Mathematica® resolved numerically the function $M(\theta,t)$, for all angles and times.

From $M(\theta,t)$, the ratio of fluorescence between the two vesicles is easily derived:

$$R(\theta,t) = \frac{C_0 - M(\theta,t)}{3\times C_0 + M(\theta,t)}\,.$$

For comparison between the model and the experimental ratios of fluorescence, $R(\theta,t)$ were calculated at $\theta$ corresponding to the center of the rectangular selection chosen for quantification (see Sect. 2.4).

The variation along the $\theta$ coordinate of fluorescence density at fixed time, although predictable in our model, proved difficult to fit with experiment because of quantification problems.

The necessities of simplification for numerically solving the diffusion model restricted us to the case of vesicles' couple of equal radius.

## References


1. T. Weber *et al.*, Cell **92**, 759 (1998).
2. S.M. Small, *The Physical Chemistry of Lipids. From Alkanes to Phospholipids* (Plenum Publishing Corporation, New York, 1986).
3. J.A. McNew *et al.*, J. Cell Biol. **150**, 105 (2000).
4. W. Almers, F.W. Tse, Neuron **4**, 813 (1990).
5. P. Durrer *et al.*, J. Biol. Chem. **271**, 13417 (1996).
6. R. Jahn, T.C. Südhof, Annu. Rev. Biochem. **68**, 863 (1999).
7. L. Yang, H.W. Huang, Science **297**, 1877 (2002).
8. B.R. Lentz, J.K. Lee, Mol. Membr. Biol. **16**, 279 (1999).
9. W. Helfrich, R.-M. Servuss, Nuovo Cimento D **3**, 137 (1984).
10. J. Israelachvili, *Intermolecular and Surface Forces* (Academic Press, San Diego, 1985).
11. L. Lis *et al.*, Biophys. J. **37**, 667 (1982).
12. R.P. Rand, V.A. Parsegian, Biochim. Biophys. Acta **988**, 351 (1989).
13. F. Pincet, L. Lebeau, S. Cribier, Eur. Biophys. J. **30**, 91 (2000).
14. F. Pincet *et al.*, Phys. Rev. Lett. **73**, 2780 (1994).
15. E. Perez *et al.*, Eur. Phys. J. B **6**, 1 (1998).
16. R.L. Ornberg, T.S. Reese, J. Cell Biol. **90**, 40 (1981).
17. M.M. Kozlov, L.V. Chernomordik, Biophys. J. **75**, 1384 (1998).
18. P.I. Kuzmin, J. *et al.*, Proc. Natl. Acad. Sci. USA **98**, 7325 (2001).
19. L. Lebeau *et al.*, Chem. Phys. Lipids **62**, 93 (1992).
20. M.I. Angelova *et al.*, Progr. Colloid Polym. Sci. **89**, 127 (1992).
21. L. Mathivet, S. Cribier, P.F. Devaux, Biophys. J. **70**, 1112 (1996).
22. R. Kwok, E. Evans, Biophys. J. **35**, 637 (1981).
23. M. Arrio-Dupont *et al.*, Biophys. J. **70**, 2327 (1996).
24. E. Evans *et al.*, Science **273**, 933 (1996).
25. T.J. McIntosh, D. Magid, in *Phospholipids Handbook*, edited by G. Cevc (Dekker, New York, 1993).
26. C. Helm, J.N. Israelachvili, P. Mc Guiggan, Biochemistry **31**, 1794 (1992).
27. T. Kuhl *et al.*, Langmuir **12**, 3003 (1996).
28. S.A. Safran, T.L. Kuhl, J.N. Israelachvili, Biophys. J. **81**, 659 (2001).
29. L. Chernomordik *et al.*, Biophys. J. **69**, 922 (1995).
30. D. Siegel, Biophys. J. **65**, 2124 (1993).
31. E. Evans, D. Needham, J. Phys. Chem. **91**, 4219 (1987)
32. R.J. Rubin, Y. Chen, Biophys. J. **58**, 1157 (1990).
33. L.K. Tamm, H.M. McConnell, Biophys. J. **47**, 105 (1985).
34. H.C. Berg, E.M. Purcell, Biophys. J. **20**, 193 (1977).
35. V. Marchi-Artzner *et al.*, J. Phys. Chem. **100**, 13844 (1996).
36. F.S. Cohen *et al.*, J. Cell Biol. **98**, 1054 (1984).
37. G.B. Melikyan, J.M. White, F.S. Cohen, J. Cell Biol. **131**, 679 (1995).